DISCRETE PREISACH MODEL FOR THE SUPERELASTIC RESPONSE OF SHAPE MEMORY ALLOYS

A Thesis

by

SRIKRISHNA DORAISWAMY

Submitted to the Office of Graduate Studies of
Texas A&M University
in partial fulfillment of the requirements for the degree of

MASTER OF SCIENCE

December 2010

Major Subject: Mechanical Engineering

DISCRETE PREISACH MODEL FOR THE SUPERELASTIC RESPONSE OF SHAPE MEMORY ALLOYS

A Thesis

by

SRIKRISHNA DORAISWAMY

Submitted to the Office of Graduate Studies of
Texas A&M University
in partial fulfillment of the requirements for the degree of

MASTER OF SCIENCE

Approved by:

Chair of Committee,	Arun R. Srinivasa
Committee Members,	Raymundo Arroyave
	William Rundell
Head of Department,	Dennis O'Neal

December 2010

Major Subject: Mechanical Engineering

ABSTRACT

Discrete Preisach Model for the Superelastic Response of Shape Memory Alloys.

(December 2010)

Srikrishna Doraiswamy, B. Tech., Indian Institute of Technology;

Chair of Advisory Committee: Dr. Arun R. Srinivasa

The aim of this work is to present a model for the superelastic response of Shape Memory Alloys (SMAs) by developing a Preisach Model with thermodynamics basis. The special features of SMA superelastic response is useful in a variety of applications (eg. seismic dampers and arterial stents). For example, under seismic loads the SMA dampers undergo rapid loading–unloading cycles, thus going through a number of internal hysteresis loops, which are responsible for dissipating the vibration energy. Therefore the design for such applications requires the ability to predict the response, particularly internal loops. It is thus intended to develop a model for the superelastic response which is simple, computationally fast and can predict internal loops. The key idea here is to separate the elastic response of SMAs from the dissipative response and apply a Preisach Model to the dissipative response as opposed to the popular notion of applying the Preisach Model to the stress–strain response directly. Such a separation allows for the better prediction of internal hysteresis, avoids issues due to flat/negative slopes in the stress–strain plot, and shows good match with experimental data, even when minimal input is given to the model.

The model is developed from a Gibbs Potential, which allows us to compute a driving force for the underlying phase transformation in the superelastic response. The hysteresis between the driving force for transformation and the extent of transformation (volume fraction of martensite) is then used with a Preisach model. The

Preisach model parameters are identified using a least squares approach. ASTM Standards for the testing of NiTi wires (F2516-07$^{\varepsilon 2}$), are used for the identification of the parameters in the Gibbs Potential. The simulations are run using MATLAB ®. Results under different input conditions are discussed. It is shown that the predicted response shows good agreement with the experimental data. A couple of attempts at extending the model to bending and more complex response of SMAs is also discussed.

TABLE OF CONTENTS

CHAPTER Page

LIST OF TABLES

LIST OF FIGURES

FIGURE Page

CHAPTER I

INTRODUCTION

Shape memory alloys (SMAs) belong to a special class of materials which are able to show near-complete strain recovery of strain under thermal and mechanical loading cycles. The two key features observed in SMA are the *shape memory effect* and the *pseudoelastic effect* also known as the *superelastic effect*. These two effects arise from solid-solid phase transformations between austenite and martensite phases in such materials [4]. The phenomenon in which the material recovers all the deformation when heated above a certain temperature (known as A_f), after having deformed at a lower temperature, is called the *shape memory effect*, whereas the phenomenon where the material undergoes large strains (of the order of 10%) which are recoverable on unloading is known as the *superelastic effect*.

A. Shape Memory Effect and Superelastic Effect

Shape memory alloys exhibit the features mentioned above due to phase transformations between the austenite (high temperature phase/high stress) and martensite (low temperature phase/low stress) phases. Typically, SMAs have four characteristic transformation temperatures at stress-free state, M_s, M_f, A_s, A_f. M_s signifies the starting of the martensite phase formation (austenite $\rightarrow$ martensite) and M_f marks the end of this transformation. Similarly, in the reverse transformation (martensite $\rightarrow$ austenite) A_s and A_f mark the start and end of the transformation to austenite. The difference in crystal structures of austenite and martensite phases is the origin for the shape memory effect and the superelastic effect.

The journal model is *IEEE Transactions on Automatic Control*.

1. Shape Memory Effect

The shape memory effect is observed when the material originally at a temperature below M_f is deformed and when unloaded shows a persistent strain. From this state, when the SMA is heated above A_f it completely recovers the original "shape" and reverts to the zero strain state. The schematic of shape memory effect is shown in a stress–strain–temperature plot in Fig. 1.

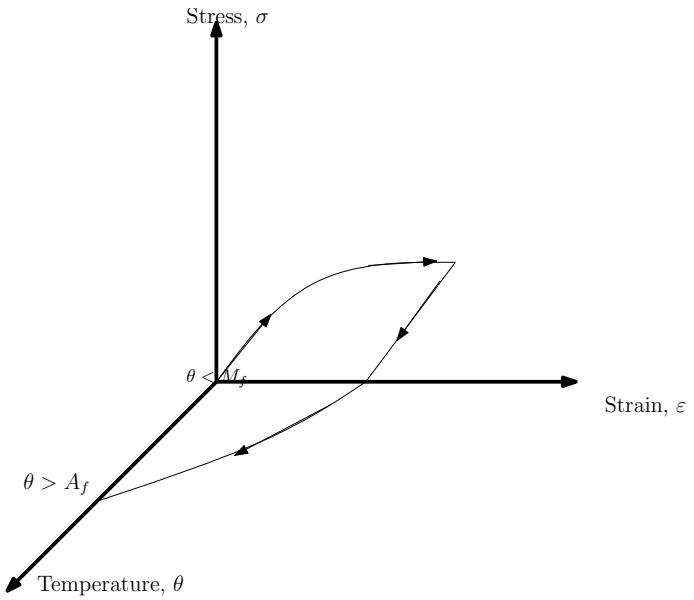

Fig. 1. Schematic of a typical load-temperature cycle for the shape memory effect

2. Superelastic Effect

Shape memory alloys, when deformed to large strains (about 10%) at a constant temperature (above A_f), completely recover the strain on unloading. The large strain are inelastic and induced by phase transformation. The superelastic response, though with no apparent plastic strain, still shows a large hysteresis. Therefore the superelastic effect has two different applications: one where the large recoverable strains are taken advantage of, and the other where the large hysteresis is used to dissipate

energy (for e.g. vibration damping). The schematic of superelastic response on an isothermal stress-strain plot is shown in Fig. 2.

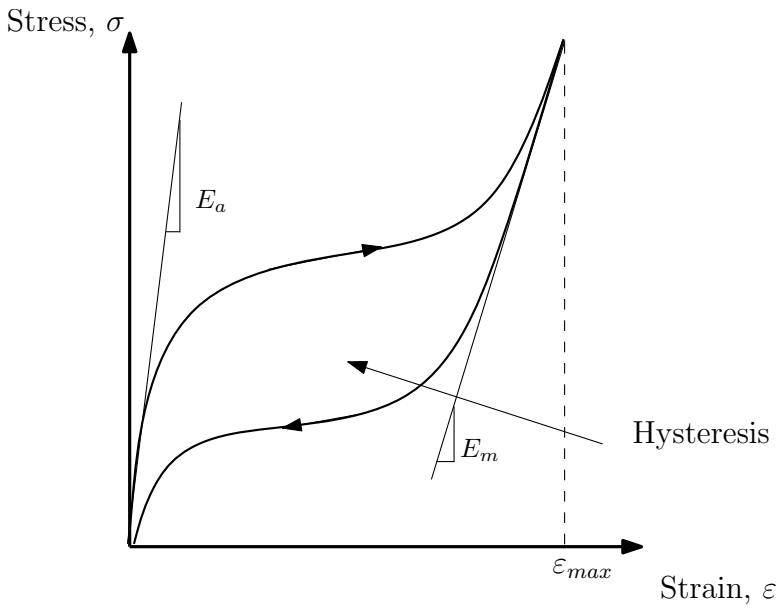

Fig. 2. Superelastic effect : Schematic of a typical stress–strain response at constant temperature

The applications of shape memory alloys, particularly using its superelastic property range from vibration damping in civil engineering structures [5, 6] to morphing wings in aerospace engineering [7] and dentures and stents for medical applications [8, 9]. For almost all of the uses of shape memory alloys, a good understanding of the material, combined with predictive capability of its response will improve its usability. To this end, there have been works by many material scientists [10, 11, 12] to understand the properties of SMAs and a number of models for the superelastic and the shape memory response[13, 14, 15] of SMAs. Recently, there have also been numerous attempts to create new shape memory alloys to perform at high temperatures[16, 17, 18, 19] and show memory effects under magnetic conditions [20, 21]

Some of the salient features that are to be noted in the SMA superelastic response are the plateau stresses, the area of hysteresis, internal loops of hysteresis, and the difference in moduli between the austenite and martensite phases. The regions in the stress–strain response plot which shows very small change in stress with a large change in strain, while loading and unloading are called the plateau stresses. ASTM standards for testing of NiTi (F2516-07$^{\varepsilon 2}$) shows that these can be computed to be the stress corresponding to 2.5% strain while loading and the stress corresponding to 3% stress while unloading. The area of hysteresis gives an idea of the dissipation, which can be used to dampen vibrations [5] and the large hysteresis in combination with stiffness differences in the material allows us to use the material for making stents [9].

The modeling of shape memory alloys (SMAs) has been primarily in two different ways, models which are analogous to elastoplasticity [15, 13, 22, 23, 24] and those which are analogous to ferromagnetic domain wall models [25, 26, 27]. The plasticity models assume that the phase transformations are similar to plastic flow. Under this assumption, flow rules, yield conditions, normality conditions etc., are developed for the phase transformation in such models. While these models have firm thermodynamic foundations, plasticity based models require extensive modifications to the flow rule in order to account for internal loops.

On the other hand, models based on magnetic hysteresis, such as domain wall models, free energy based models [28, 26] and Preisach models [29, 30, 31, 32, 33] exploit an analogy of shape memory alloy phase transformations to magnetic domain wall transitions. The key idea here is that the models compare the superelastic hysteresis to the magnetic hysteresis. Such models are extremely versatile and capable of modeling inner loops and other complex phenomena in a fairly straightforward way[25]. The mathematical theory of Preisach models is also well developed with

several rigorous results [1, 34]. A special discussion of a few Preisach type models is undertaken in Chapter III.

B. Motivation and Scope

Based on the literature study, **it is intended to develop a model for the superelastic response which is simple, computationally fast, and can predict internal loops.** In order to do this we choose a Preisach type model for the hysteresis. The idea of the Preisach model is to divide the material into a large number of small "cells" called hysterons. Each cell can switch between an austenitic and a martensitic phase. The cells differ in their thermodynamic driving force required to switch them from the austenite to the martensite phase and vice versa. The response of the entire RVE is the superposition of the response of the cells. But, instead of applying the hysteresis model directly to the stress–strain response, we will introduce a driving force for the phase transformation through an appropriate choice of Gibbs Potential, and apply the Preisach model to the hysteresis between the driving force for transformation and the martensite volume fraction. The key idea is to separate the thermoelastic response from the actual dissipative mechanism, so that the Preisach type models are used to model the physical dissipation mechanism rather than the phenomenological "hysteresis". This considerably simplifies the response of the material. We will also elucidate direct methods to obtain parameters for the model in order to avoid ad hoc fitting of model parameters.

Moreover in a design setting, it is important for designers to have an idea of approximate stresses for preliminary designs, without adequate experimental data. Therefore it is also intended to provide the possibility to use the model for such design proposes (e.g. to calculate the amount of heat dissipated and approximately

calculate stress at a particular strain, given limited experimental data).

CHAPTER II

MODEL DEVELOPMENT

We will now detail the steps involved in developing a model for the superelastic response of shape memory alloys. As mentioned earlier, to model such a response, it is proposed to carefully separate the elastic response from the inelastic response. In order to do this in a systematic way, we first choose a Gibbs Potential which models the thermoelastic response of the SMA. Based on this Gibbs Potential, we invoke the power theorem to compute the dissipation, from which we obtain the driving force for the phase transformation. Once we have the relation between the driving force of transformation and the volume fraction of martensite produced, we will reduce the stress–strain data (from, for example, Fig. 3) to driving force–volume fraction data and then develop the Preisach Model for this hysteretic response.

A. Thermodynamic Framework

Consider a shape memory alloy wire AB, of initial length L_0 along the X-axis. Let end A be fixed, and end B be subjected to an axial force of F. If the initial cross-sectional area is A, then the axial referential stress is given by $\sigma = \frac{F}{A}$. The strain in the material (assumed to deform homogeneously) is given by $\varepsilon = \frac{L_0 - L}{L}$, where L is the current length of the wire.

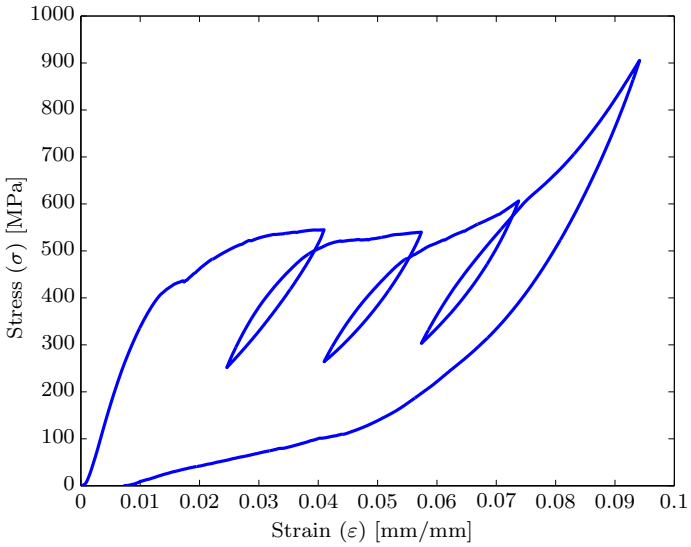

Fig. 3. A typical superelastic response of an untrained Ni-Ti SMA wire, with an internal loop

1. The Gibbs Potential

We seek to model the response of shape memory alloy wires under uniaxial tension by introducing a Gibbs potential per unit volume (inspired from [15]) which is assumed to be a function of the stress σ, temperature θ and the extent of transformation (or volume fraction of martensite formed during phase transition), α. The Gibbs potential will pave the way to arrive at a driving force expression for the phase transformation. Specifically the Gibbs potential energy per unit reference volume is assumed to be of the form,

$$G = -\left(\frac{\alpha\sigma^2}{2E_m} + \frac{(1-\alpha)\sigma^2}{2E_a}\right) + B\alpha(\alpha-1) + (1-\alpha)(a+b\theta) - C\theta(1-\log\theta) \quad (2.1)$$

where α is the martensite volume fraction, σ is the stress, B, a, b are constants, C is the specific heat, θ is the temperature, E_a and E_m are the austenitic and marten-

sitic elastic moduli. The constant B represents the interaction energy between the austenite and martensite phases [15] while constants a and b represent the latent heat difference between the austenite and martensite phases.

2. The Driving Force

From classical thermodynamics, we know that the entropy is given by,

$$\eta = -\frac{\partial G}{\partial \theta}, \tag{2.2}$$

and the elastic strain is given by,

$$\varepsilon_e = -\frac{\partial G}{\partial \sigma} = \frac{\alpha\sigma}{E_m} + \frac{(1-\alpha)\sigma}{E_a}. \tag{2.3}$$

Also, we know that the Helmholtz potential ψ, is related to Gibbs potential G, by,

$$\psi = G - \sigma\frac{\partial G}{\partial \sigma} \tag{2.4}$$

Invoking the power theorem, the difference between the rate of external working and the rate of change of the Helmholtz potential, at constant temperature, must be equal to the rate of the energy dissipated i.e the heating.

In other words,

$$\textit{the dissipation rate}(\xi) = \tag{2.5}$$
$$\textit{external working } (\sigma\dot{\varepsilon}) - \textit{rate of change of Helmholtz potential at const. temp.}(\dot{\psi}|_\theta)$$

Using Eqns. (2.3), (2.4) and simplifying the above, we get,

$$\sigma(\dot{\varepsilon} - \dot{\varepsilon}_e) - \frac{\partial G}{\partial \alpha}\dot{\alpha} = \xi \tag{2.6}$$

From Eqn. (2.6) we observe that there are two contributions to the rate of dissipation, one from the shape change that occurs due to phase transition ($\sigma(\dot{\varepsilon}-\dot{\varepsilon}_e)$) and the other from the energy difference between the two phases ($-\frac{\partial G}{\partial \alpha}\dot{\alpha}$). It is natural to assume that the elongation due to phase transformation is proportional to the extent of transformation and the maximum transformation strain, ε_{max} which is of the order of 6% for Ni-Ti, i.e. we will stipulate that

$$\dot{\varepsilon} - \dot{\varepsilon}_e = \varepsilon_{max}\dot{\alpha} \Rightarrow \varepsilon - \varepsilon_e = \varepsilon_{max}\alpha \tag{2.7}$$

where α is the volume fraction of martensite evolved at strain, ε.

In the above equation note that, when $\alpha = 1$, $\varepsilon - \varepsilon_e = \varepsilon_{max}$ and when $\alpha = 0$, $\varepsilon - \varepsilon_e = 0$. Now substituting Eqn. (2.7) into Eqn. (2.6).

$$\left(\sigma\varepsilon_{max} - \frac{\partial G}{\partial \alpha}\right)\dot{\alpha} = \xi \tag{2.8}$$

We can now identify the driving force for the phase transformation in the superelastic response of the SMA:

$$\mathcal{F} = \sigma\varepsilon_{max} - \frac{\partial G}{\partial \alpha} \tag{2.9}$$

Until this stage, we have followed a thermodynamical framework that is commonly used for phase transforming materials. If one were to follow a plasticity like model , one will develop an evolution equation for α, which would be the counterpart for the flow rule for the plastic strain in classical plasticity. Here we will follow a different approach. ***We are going to use a Preisach model (to be described shortly) for the relationship between driving force $\mathcal{F}$ and volume fraction,*** α.

Notice that this particular method for using the Preisach Model, is different from

the conventional approach for Preisach Models applied to SMA hysteresis, where the stress–strain or temperature–strain relationships are directly modeled with Preisach elements. The advantages of the proposed method will become clear shortly.

3. Driving Force and Volume Fraction from Experimental Data

As mentioned in the previous section, the proposed method uses the relationship between the driving force $\mathcal{F}$ and volume fraction α for the Preisach Model. To this end, the following develops the required relations.

From the previous sections, Eqns. (2.1) and (2.9) show that the driving force is given by:

$$\mathcal{F} = \sigma\varepsilon_{max} + \sigma^2\left(\frac{1}{2E_m} - \frac{1}{2E_a}\right) - B(2\alpha - 1) + a + b\theta \tag{2.10}$$

It is important to note that, here the driving force is a function of stress, temperature and the volume fraction. Thus in this model, temperature effects are accounted for in the driving force itself. Before we proceed, we nondimensionalize the variables. In order to do this, we identify a typical stress σ_0, a typical strain ε_0 and a typical temperature θ_0. Now, we write the nondimensionalized variables, $\sigma^* = \sigma/\sigma_0$, $\varepsilon^* = \varepsilon/\varepsilon_0$, $\theta^* = \theta/\theta_0$.

Henceforth, we will drop the $*$'s from the nondimensionalized variables for better readability.

We observe that from Eqns. (2.3), (2.7) and (2.10), that given experimental data for stress and strain, one can use the framework developed up to now to compute the driving force ($\mathcal{F}$) and the volume fraction of the martensite phase (α). Indeed, using Eqns. (2.3) and (2.7) gives us,

$$\alpha = \frac{\varepsilon - \dfrac{\sigma}{E_a}}{\dfrac{\sigma}{E_m} - \dfrac{\sigma}{E_a} + 1} \tag{2.11}$$

B. Data Reduction

Now that we have a set of equations for the driving force for the transformation and the martensite volume fraction as a function of the stress, the strain, and the temperature, we can use experimental data from a stress-strain plot and derive the driving force for transformation and the martensite volume fraction.

$$\mathcal{F} = \sigma\varepsilon_{max} + \sigma^2\left(\frac{1}{2E_m} - \frac{1}{2E_a}\right) - B(2\alpha - 1) + a + b\theta \tag{2.12a}$$

$$\alpha = \frac{\varepsilon - \dfrac{\sigma}{E_a}}{\dfrac{\sigma}{E_m} - \dfrac{\sigma}{E_a} + 1} \tag{2.12b}$$

Using Eqns. (2.12a), (2.12b) we convert every data point in an isothermal $\sigma - \varepsilon$ plot to a $\mathcal{F} - \alpha$ plot. Indeed, Fig.(4(b)) shows the conversion of the experimental data given in Fig.(3). It can be seen that the hysteresis curve does not have any flat plateaus and resembles a typical ferromagnetism hysteresis curve (see, for eg., Fig. (1.1) in [35]). Such a data reduction is therefore useful to apply a conventional hysteresis model (such as those used to model ferromagnetic hystereses) to Shape Memory Alloy hysteresis.

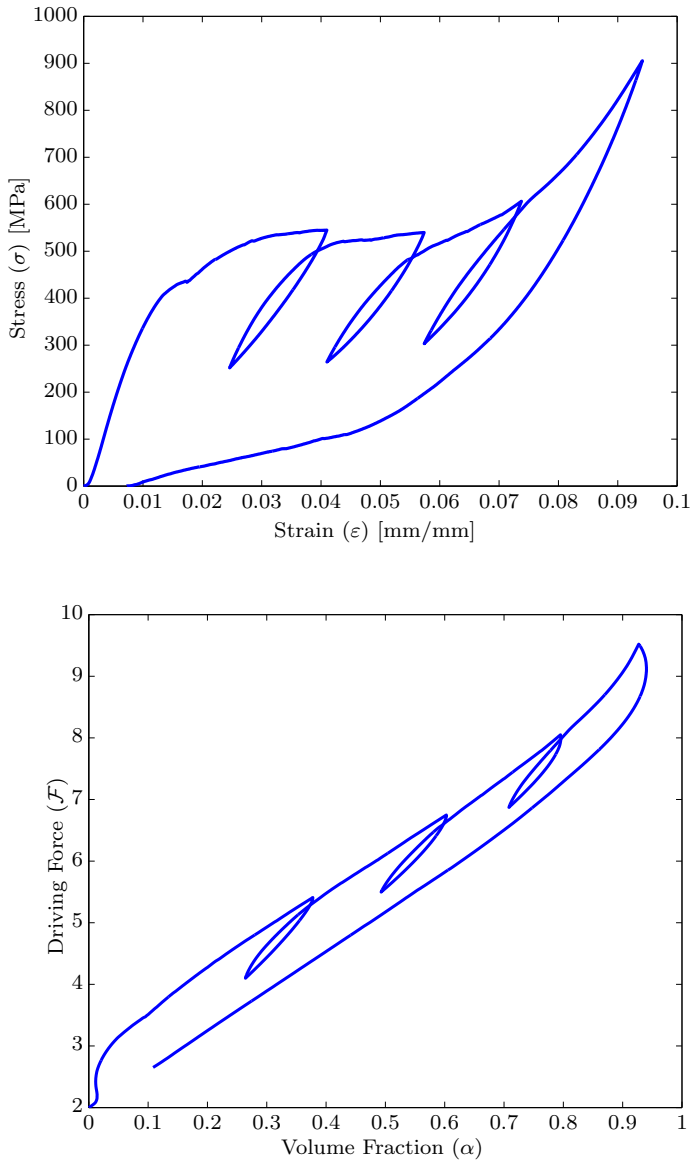

Fig. 4. The driving force $\mathcal{F}$ vs. volume fraction α plot for the experimental data shown in Fig. 3. Notice that the hysteresis looks more like a magnetic hysteresis after the data reduction, with the characteristic S shape (as can be seen in pg. 5 in [1])

CHAPTER III

THE PREISACH MODEL

In the last chapter, we detailed the data reduction that is required to separate the dissipative part of the response from the elastic response. This was done by choosing a Gibbs Potential and using the power theorem to derive a driving force for the phase transformation. In this chapter, we will see what the Preisach model is, how it models hysteresis, and why the Preisach model is a good choice to model the superelastic response of Shape Memory Alloys.

A. Introduction

The Preisach model was originally intended for magnetic materials, when it was first introduced by F.Preisach in 1935. It was first presented "as a superposition of elementary kernels termed hysterons" [4]. In his book, "Mathematical Models of Hysteresis", Mayergoyz [36] has noted that D.H. Everett developed a hysteresis model similar to the Preisach model for adsorption hysteresis [37]. The central idea is to replace a smooth hysteresis curve with a set of steps. Each step is modeled as a "hysteron" and is parameterized by three values: the 'on' condition, the 'off' condition and the height of the step. Hysteresis curves are represented as superpositions of such elemental steps.

Consider a set of such "units of hysteresis" or "hysterons" $\hat{\gamma}_{\alpha\beta}$. Each of these units can be represented as a non-ideal switch on the input-output diagram (See Fig 5). α and β are numbers which correspond to the switch on, and switch off values. It is assumed that $\alpha \geq \beta$. The output of the hysteron is assigned as +1 and -1. This can be represented as $\hat{\gamma}_{\alpha\beta}u(t) = +1$ and $\hat{\gamma}_{\alpha\beta}u(t) = -1$ for the "on" and "off" states (outputs) respectively. If for example that input is increased, the path taken

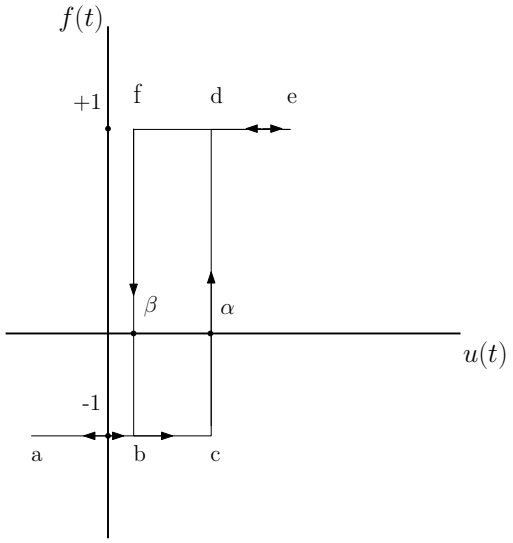

Fig. 5. The hysteron for the classical Preisach model. Note that α and β are the switching values for this hysteron and the arrows point the allowable paths corresponding to changes in input

would be *abcde* in Fig. 5 and when the input is decreased, the path *edfba* is taken. Along with the switch values $\hat{\gamma}_{\alpha\beta}$, a weight function $\mu(\alpha, \beta)$ is also used to model the hysteresis. The Preisach model can now be written as below:

$$f(t) = \iint_{\alpha \geq \beta} \mu(\alpha, \beta) \hat{\gamma}_{\alpha\beta}[u(t)] \, \mathrm{d}\alpha \, \mathrm{d}\beta \tag{3.1}$$

The representation above is for a infinite set of hysterons. But it is possible to use this setup for a finite set of hysterons to make it computationally easy and fast. The setup for such a "Discrete Preisach Model" will be discussed in Section C.

B. Survey of Existing Preisach Type SMA Models

In the recent past, papers presenting Preisach Model for hysteresis of smart materials (shape memory alloys and piezoelectrics, in particular) are by Ortín [30], Hughes and

Wen [29], and Bo and Lagoudas [14].

Preisach models have been used in the modeling of SMAs in primarily two ways. One is using Preisach models to predict the temperature-strain hysteresis [33, 29, 14] and the other is to predict the stress-strain or force-displacement hystereses in SMAs [32, 30].

In the paper by Bo et al., [14], a number of hysteresis models for Shape Memory Alloy modeling have been discussed including Duhem-Madelung model, Preisach model, and K-P type models. In particular, the Preisach model was used for modeling the temperature-strain hysteresis. The paper shows how the integral type Preisach model can be used to model the major and minor hysteresis loops. The integral type Preisach Model is developed by choosing a distribution function $\mu(T_\alpha, T_\beta)$ for the martensite volume fraction, ξ, where T_α and T_β are the hysteron parameters for the hysteron, $\gamma_{\alpha\beta}$. The total volume fraction is given by:

$$\xi[T] = \iint\limits_{T_\alpha \geq T_\beta} \mu(T_\alpha, T_\beta)\gamma_{\alpha\beta} T \ \mathrm{d}T_\alpha \mathrm{d}T_\beta \tag{3.2}$$

The paper also lists the disadvantages of using a Preisach model to SMA hysteresis modeling, especially the difficulty in incorporating effects due to training and different loading paths.

In [30], Ortín presents a model for the stress-strain hysteresis of SMA wires. This model uses the integral Preisach approach and the applied stress is the forcing variable and the output variable is the strain (both functions of time). As with the classical Preisach model we have the equation that gives the strain, $\varepsilon(t)$ as an integral over all the hysterons, $\gamma_{\alpha\beta}$,

$$\varepsilon(t) = \iint\limits_{\alpha \geq \beta} \mu(\alpha, \beta)\gamma_{\alpha\beta}\sigma(t) \ \mathrm{d}\alpha \mathrm{d}\beta \tag{3.3}$$

Here, the strain can be computed from the experimental data by considering "first order reversal paths, i.e.,a path that is obtained from the main loading branch on unloading at a given σ value".

However current Preisach models for shape memory alloys suffer from a number of drawbacks:

1. The models are generally not thermodynamically based, but rather purely phenomenological in nature.

2. Most Preisach type models have focused on either purely thermal [33, 14] or purely mechanical response [30]. However if the hysteresis loop changes with temperature, all the forward and backward transformation functions need to be modified as functions as temperature, which makes them extremely complicated.

3. Many controls systems applications based on cancellation of non-linearity, require inversion of the models [38]. This is not easy to do with a simple Preisach model, although for certain modifications of the Preisach models techniques are available.

4. For Nitinol wires, it is possible that the stress-strain response shows a non-hardening or in some cases a softening response, i.e. the slope of the stress-strain graph may be zero or even slightly negative. It is not possible to use a Preisach model to directly simulate this, because strain controlled experiments cannot be modeled this way.

C. The Discrete Preisach Model

In Section A, a brief idea about the classical Preisach model was discussed. In this section we will analyze the Discrete Preisach Model, the discrete analog of the Clas-

sical Preisach Model. Here again, the model is setup as an ensemble of N hysterons, each of which looks like the one shown in Fig.6. Each hysteron (Fig. 6) is basically a non-ideal switch that switches on when the driving force (or input), F increases beyond $F_{forward}$, giving an output $\Delta\alpha$ and switches off at $F_{backward}$. It is to be noted that once the driving force crosses the $F_{forward}$ (while *increasing* the driving force), the output does not change when the driving force is further increased. Similarly, when the driving force crosses $F_{backward}$ (while *decreasing* the driving force) the output stays at zero. To model the driving force for phase transformation-volume fraction of martensite hysteresis, we will use a large number of such hysterons which switch on and off at different values of the input force, each contributing to the output.

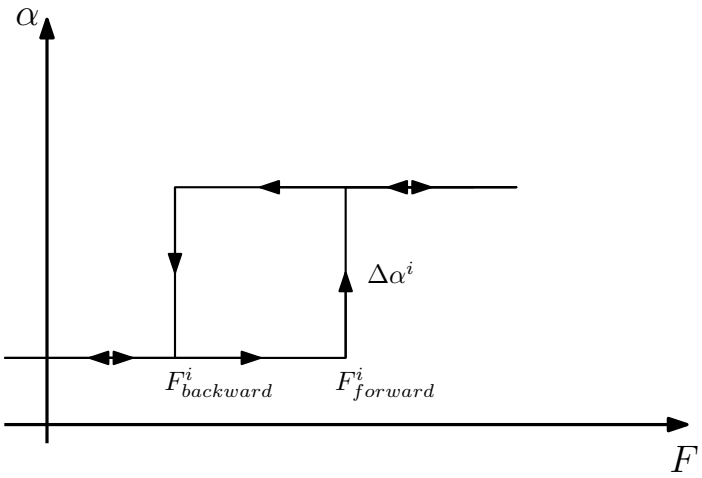

Fig. 6. The hysteron or basic hysteretic element used in the Preisach model. Note that the directions of allowed transformations are indicated by the arrows on the hysteron. Also note that $\Delta\alpha^i$ is positive $\forall\ i$.

1. Setting up the Preisach Model

To setup the Discrete Preisach model for our model, we will list the requirements for the hysterons. In this context, we first describe the modus operandi for use of Preisach Model with the thermodynamic model presented in Chapter II. To reiterate, the

hysteresis we model is the driving force for phase transformation vs. volume fraction of martensite hysteresis presented in Eqns. (2.12a), (2.12b) and Fig. 4(b). It is now obvious that the input for the hysteron is the driving force for phase transformation and the output is the volume fraction of martensite[1]. This immediately implies that the volume fraction output for each hysteron can either be 0 (when switched off) and $\Delta\alpha_i$ (when switched on), as shown in Fig. 6.

a. The Algorithm for Preisach Model

A state S_i of the i^{th} hysteron (of a total of N hysterons) can be one of two values, 0 or $\Delta\alpha_i$. A convenient way to consider this (for the sake of writing as programmable code), is as follows. Let $S_i^{(n)}$ be the state of the i^{th} hysteron at (pseudo) time t_n, $\mathcal{F}^{n+1}$ be the driving force at t_{n+1}, then the sum of outputs of all the hysterons at the end of time t_{n+1} is computed by the following extremely simple algorithm,

Algorithm 1 Algorithm for Discrete Preisach Model

if $S_i^{(n)} = 0$ & $\mathcal{F}^{(n+1)} > F^i_{forward}$ **then**

$S_i^{(n+1)} \leftarrow \Delta\alpha_i$

else if $S_i^{(n)} = \Delta\alpha_i$ & $\mathcal{F}^{(n+1)} < F^i_{backward}$ **then**

$S_i^{(n+1)} \leftarrow 0$

else

$S_i^{(n+1)} \leftarrow S_i^{(n+1)}$

end if

$\alpha^{(n+1)} \leftarrow \sum_{i=1}^{N} S_i^{(n+1)}$

Hence, the state of the system (i.e. the extent of transformation, given by the

[1]For the sake of brevity, "driving force" will be used in place of "driving force for phase transformation" and "volume fraction" will be used to refer to "volume fraction of martensite", henceforth.

total volume fraction of martensite evolved), is:

$$\alpha = \sum_{i=1}^{N} S_i \tag{3.4}$$

b. Obtaining the Preisach Parameters

The algorithm shows how to compute the total output given the input. But, this implies knowledge of the hysteron parameters $F_{forward}$, $F_{backward}$, $\Delta\alpha$. For a given stress-strain data, once the driving force–volume fraction is computed, we need to compute the hysteron parameters, so that we can find the hysteron output, given an input. In order to do this, we describe a convenient way of arranging hysterons in a triangle, the reason for which will become evident shortly.

c. Preisach Triangle

The Preisach Triangle (pp. 32-39 [36]) is a convenient approach to arranging the hysterons. The hysterons are assigned the driving forces in a triangle (see Fig.7(a)), so that the hysterons with the lowest forward driving force are at the bottom of the triangle and the hysterons with highest forward driving force are arranged at the top of the triangle[2]. Similarly, the hysterons with the lowest backward driving force are arranged at the left end of the triangle and the hysterons with the highest backward driving force are arranged at the right end. In other words, the following lists the properties of hysterons in the Preisach Triangle.

The hysteron switch values are assigned in a way to:

- place every hysteron with a particular switch on value in the same row in an "upper-triangle" (Fig. 7).

[2]Highest and lowest driving force are the maximum and minimum values of the driving force computed using Eqn. (2.12a)

- place every hysteron with a particular switch off value in the same column.
- place hysterons in an increasing order (left to right) of switch off value in every row of the triangle.
- place hysterons in a increasing order (bottom to top) of switch on values in every column of the triangle.

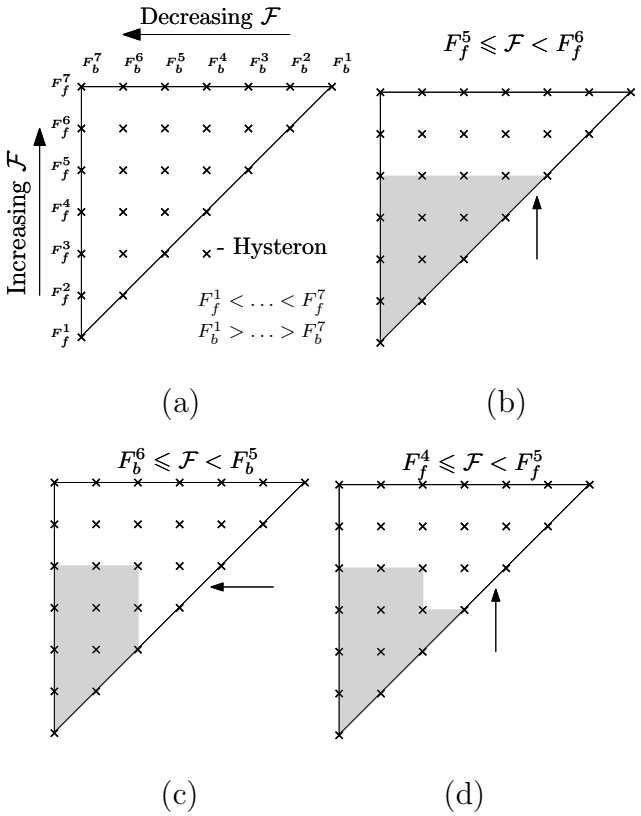

Fig. 7. (a) The Preisach triangle is a convenient way of assigning hysterons with their parameters to allow systematic switch on and switch off of the hysterons. Note that the directions of sweep are marked on the figure. (b),(c),(d) An example of the sequence of states in the Preisach triangle is shown. The grayed portion of the triangle includes hysterons which are switched on. The value of the driving force which enforces the state is shown at the top of each state.

It can now be seen that, if one were to increase the input, the hysterons get

switched on row by row, from the bottom-most row upwards. When the input is not increased any further, it stays until any change is made to the input. If in case, the input is decreased from this state, the hysterons (which are currently switched on) switch off starting with those which have the highest (relative to the current input) switch off values (which would be the right most column of hysterons of all those which are currently switched on). Progressively, the hysterons will switch off column-by-column, right to left. A particular cycle can be better visualized by looking at Fig. 7.

An interesting point to note here is that, by assigning the hysterons to specific positions in the triangle, we have already taken care of finding two of the the three parameters per hysterons. Now to use Algorithm 1, all we need to do is to compute the output per hysteron. Once this is done, we will have a complete, Preisach prediction of the hysteresis of driving force–volume fraction (Fig. 4(b)).

Returning to the Preisach triangle, let us consider a Preisach triangle with n hysterons on its side. It is clear that the total number of hysterons in the triangle is $\frac{1}{2} \times n \times (n+1)$. It thus follows that, the number of unknowns (hysteron outputs, or $\Delta\alpha_i$) that we need to solve is $\frac{n(n+1)}{2}$. We will setup a system of equations to solve for these unknowns.

d. Solving for the $\Delta\alpha_i$ of Hysterons

Setting up the system of equations to solve the output parameter of the hysteron is better understood through an example. Let us consider the example shown in 7. We have a Preisach triangle with 28 hysterons (side is 7). Therefore the number of unknowns here is 28. Now, let us assume that the points (say, $k < 28$) on the hysteresis data is as follows.

$$F = \begin{bmatrix} 0 \\ \vdots \\ \mathcal{F}_1 \\ \vdots \\ \mathcal{F}_2 \\ \vdots \\ \mathcal{F}_3 \\ \vdots \end{bmatrix}_{k\times 1} \qquad \alpha = \begin{bmatrix} 0 \\ \vdots \\ \alpha_1 \\ \vdots \\ \alpha_2 \\ \vdots \\ \alpha_3 \\ \vdots \end{bmatrix}_{k\times 1}$$

Now, obviously, since the first entry is 0, none of the hysterons are switched on. This is indeed 7(a). Let us assume that, after a few steps, the state of the hysterons is given by 7(b). Let $\mathcal{F}_1$ be the driving force corresponding to this state, (which is therefore $F_f^5 \leq \mathcal{F}_1 < F_f^6$) and α_1 be the volume fraction that has evolved at this state. Clearly, the hysterons which contribute to α_1 are the hysterons which are in the grayed out area. Thus, we can write

$$\begin{aligned} \Delta\alpha_{11}+\Delta\alpha_{21} + \Delta\alpha_{22} + \Delta\alpha_{31} + \Delta\alpha_{32} + \Delta\alpha_{33} + \Delta\alpha_{41} + \Delta\alpha_{42} \\ + \Delta\alpha_{43} + \Delta\alpha44 + \Delta\alpha_{51} + \Delta\alpha_{52} + \Delta\alpha_{53} + \Delta\alpha_{54} + \Delta\alpha_{55} = \alpha_1 \end{aligned} \tag{3.5}$$

where $\Delta\alpha_{ij}$ corresponds to the hysteron at the i-th row from the bottom and j-th column from the left.

Similarly, if we write the equations for α_2 corresponding to 7(c) and α_3 for 7(d) and so on, we can write the entire system as follows,

$$\underbrace{\begin{bmatrix} 0 & & & \dots & & & 0 \\ & & & \vdots & & & \\ 1 & 1 & \dots & 1 & 0 & \dots & 0 \\ & & & \vdots & & & \\ 1 & 1 & & \dots & & 1 & 1 \end{bmatrix}_{k\times 28}}_{A} \underbrace{\begin{bmatrix} \Delta\alpha_{11} \\ \vdots \\ \Delta\alpha_{55} \\ \vdots \\ \Delta\alpha_{77} \end{bmatrix}_{28\times 1}}_{x} = \underbrace{\begin{bmatrix} 0 \\ \vdots \\ \alpha_1 \\ \vdots \\ 1 \end{bmatrix}_{k\times 1}}_{\mathrm{B}} \tag{3.6}$$

Note here, that the format is the classic system of linear equations,

$$Ax = b$$

but, the dimensions of A are $k \times 28$ and given[3] $k < \frac{n(n+1)}{2}$ it is not possible to write x as $x = A^{-1}b$. This problem is solved by the technique of least squares. Especially, in this case, the constraints on the unknowns are that they have to be non-negative. This constrained least squares problem can be formally stated as below:

$$\begin{aligned} &\text{minimize } \|Ax - b\| \\ &\text{subject to} \\ &\qquad x_i > 0 \ \forall \ i = 1, ..., \frac{n(n+1)}{2} \end{aligned} \tag{3.7}$$

To solve , we used `CVX`, a MATLAB® package for specifying and solving convex problems (including such least squares problems) [39, 40].

Having done this, we now know everything about each of the hysterons and to get the predictions of the Preisach Models, we just need to apply Algorithm 1. In the following chapter, the details of obtaining the stress–strain hysteresis prediction

[3]Typically, the number of hysterons is more than the number of data points

from the application of Algorithm 1 and associated specifications for simulations will be presented.

CHAPTER IV

SIMULATION

In this chapter, we will detail the method by which the response of the superelastic SMA is simulated, and why the predicted response is useful. At the end of the previous chapter, we were at a stage where we knew the entire set of parameters for the hysterons. We also were able to simulate the driving force–volume fraction hysteresis based on Algorithm 1. Currently, the last piece of work left is to once again convert this predicted hysteresis to the conventional stress–strain hysteresis so that we can use the model effectively.

A. Driving Force – Volume Fraction to Stress – Strain

To compute the stress in a superelastic wire, at a constant temperature, given the strain and the set of parameters which define the hysterons, we first list the necessary equations and then elaborate the scheme that is used to perform the computation.

Let there be N hysterons each contributing α_i to the volume fraction through the Preisach setup. We note that Algorithm 1 gives,

$$\alpha = \sum_{i=1}^{K} \alpha_i \tag{4.1}$$

where $\alpha_i \; \forall \; i = 1, 2, \ldots, K$ denotes the value of the volume fraction contribution of those hysterons which are switched on at this timestep.

Now, Eqn. (2.12b) can be rewritten with σ on the left hand side,

$$\sigma = \frac{\varepsilon - \alpha}{\alpha \left(\dfrac{1}{E_m} - \dfrac{1}{E_a} \right) + \dfrac{1}{E_a}} \tag{4.2}$$

The above equations, with the addition of Eqn. (2.12a) are used for the following

scheme.

Let us assume that the information available to us at timestep t_n, is $\sigma^{(n)}$, $\varepsilon^{(n)}$, $\mathcal{F}^{(n)}$ and $\alpha^{(n)}$, where σ is the nondimensionalized stress, ε is the nondimensionalized strain, $\mathcal{F}$ is the driving force and α is the volume fraction. Also, since superelastic response is generally under isothermal conditions, the temperature θ is also known. In addition to this, we also know the strain at timestep $\varepsilon^{(n+1)}$.

We now seek to compute $\sigma^{(n+1)}$, $\mathcal{F}^{(n+1)}$ and $\alpha^{(n+1)}$.

Putting together Eqns. (4.1), (4.2), and (2.12a)

$$\alpha^{(n)} = \sum_{i=1}^{K} \alpha_i^{(n)} \tag{4.3a}$$

$$\sigma^{(n+1)} = \frac{\varepsilon^{(n+1)} - \alpha^{(n)}}{\alpha^{(n)} \left(\frac{1}{E_m} - \frac{1}{E_a} \right) + \frac{1}{E_a}} \tag{4.3b}$$

$$\mathcal{F}^{(n+1)} = \sigma^{(n+1)} + \left(\sigma^{(n+1)}\right)^2 \left(\frac{1}{2E_m} - \frac{1}{2E_a} \right) - B\left(2\alpha^{(n)} - 1\right) + a + b\theta \tag{4.3c}$$

At this stage, we use $\mathcal{F}^{(n+1)}$ to compute the updated state of the hysterons by Algorithm 1, and then we can march the time to the next step. In the following sections, we will see the details of the data used, different specifications applied to the model, and how the model is used to simulate the response of superelastic SMA , including inner loops of hysteresis and temperature effects.

B. Data Used for the Simulations

The data that is used in the majority of this work was from experiments performed by Mr. Ashwin Rao, from the Mechanical Engineering department and a member of Dr. Srinivasa's research group. The experiment was performed on 0.75 mm diame-

ter Nitinol wires purchased from Images Scientific Instruments (`www.imagesco.com`). The gauge length of the wire was 120 mm and transformation temperature around 328 K. The experiments are performed on an Instron 5567 series.

C. Model Specifications

It can be seen that the model parameters are of two kinds in the proposed model. One set of parameters are from the thermodynamical framework, from Eqn. (2.1) and the other set of parameters are the hysteron parameters. Chapter III, Section b details the procedure to obtain the parameters for the hysteron. We will now list the procedure by which the parameters in the Gibbs potential (E_a, E_m, B, a, b) are identified.

First, it is to be noted that in order to obtain the thermodynamic parameters, the entire stress–strain data is not required. We will list a few salient features of the response, corresponding to which data will have to be provided for identifying the thermodynamic parameters.

E_a and E_m are the austenitic and martensitic moduli which can be inferred directly from the plot of the response. B is the coefficent of the interfacial energy term, which is the area under the curve in the plot and a,b are parameters which are obtained by comparing responses at two different temperatures.

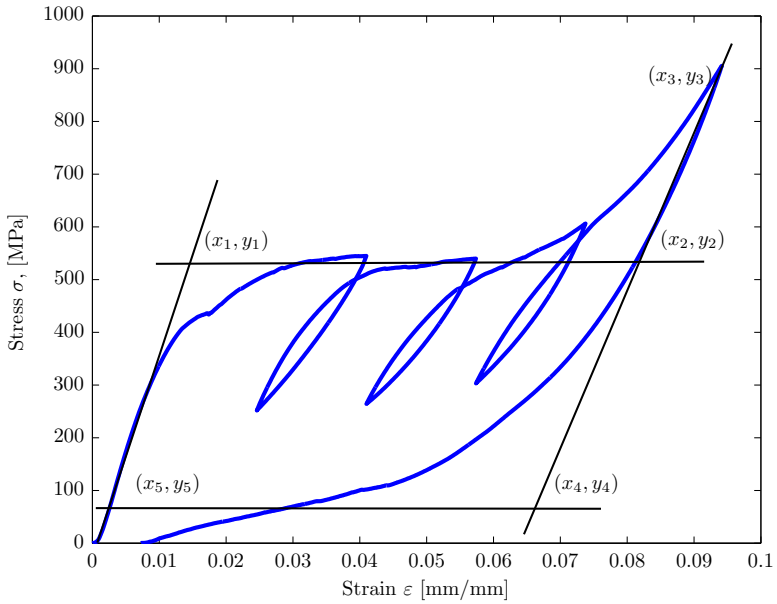

Fig. 8. The points identified for use with identification of the thermodynamic parameters from the stress–strain response. These points with two set of points (equivalent of (x_1, y_1) and (x_2,y_2)) from the response at another temperature will be used to identify the parameters.

In particular, in a given response, as shown in Fig. 8, the input given is the list of 5 points from the stress–strain response at a given temperature θ_1. The upper plateau (2.5% strain while loading, as per ASTM F2516-07$^{\varepsilon 2}$) points are (x_1,y_1) and (x_2,y_2). The lower plateau points (x_4,y_4) and (x_5,y_5) are based on 3 % strain while unloading(again, as per ASTM F2516-07$^{\varepsilon 2}$). The two slopes are tangents at the point of start of loading and the point of start of unloading. Obviously, the points mentioned above are the intersection of the slope (or "moduli") lines with the plateaus. Additionally, the points corresponding to the upper plateau, (x_1,y_1) and (x_2,y_2), at a different temperature θ_2 is also given.

Now the following list shows the method by which each of the parameters are computed. Note that the data is nondimensionalized by σ_0 (average value of stress on the line joining (x_1, y_1) and (x_2, y_2)) and ε_0 (value of strain at (x_3, y_3)).

- Moduli E_a and E_m are computed by finding the slopes of the line joining (0,0) and (x_1,y_1), and (x_3, y_3) and (x_4, y_4) respectively.
- B is negative (because of our choice of the term $B\alpha(\alpha-1)$ in the Gibbs Potential (Eqn (2.1))) of the area under the curve
- b, the thermal parameters are computed by fitting a straight line to the upper plateau values (computed as average value of stress on the line joining (x_1, y_1) and (x_2, y_2)) at temperature θ_1 and θ_2. a is a parameter which ensures that the driving force is positive and is therefore set to be 2 $|b|$

Table I. Values of nondimensional thermodynamical parameters for response shown in Fig. 8

Nondimensional Parameters	**Values**
E_a	6.92
E_m	4.95
B	-2.84
a	4.95
b	-2.47
θ_1	373
θ_2	398

D. Inputs for the Simulation

The primary input for the model is the list of points from Fig. 8 i.e. (x_i, y_i) for $i = 1, 2, \ldots, 7$. Given this input alone, a linear approximation to the experiment may be assumed and the prediction corresponding to this approximation can be predicted and is given in Chapter V.

On the other hand, if the entire experiment data is given, with the 7 points specified separately, the parameters given in Table I can still be computed the same way listed above. Additionally, the simulation can be carried out with the data points as input to the model.

E. Simulation Procedure

The following list gives a brief overview of the computer implementation of the proposed model. Appendix A.

Step 1

Obtain input data points and the strain routine to be modeled from user.

Step 2

Compute parameters, and non-dimensionalize the stress and strain data.

Step 3

Reduce data to driving force and volume fraction using Eqn. (2.12).

Step 4

Compute the Preisach hysteron parameter values for the driving force–volume fraction hysteresis obtained in Step 3.

Step 5

Once the Preisach hysteron parameters are computed, use Eqn. (4.3) to find the stress corresponding to the input strain.

CHAPTER V

RESULTS AND DISCUSSION

Setting up the simulation under the specifications listed in Chapter IV, we now look at different runs of the simulation under various cases.

A. Simulating Superelastic Response with Internal Loops of Nitinol Wire at 373 K

In this case, we use the Preisach model to simulate the experiment itself. The key points to note here are that the model has a high fidelity to the data provided. It is to be noted that, in case of the linear approximation, existing models will fare poorly, especially in capturing the plateaus. Since the proposed model fits a hysteresis to the reduced data, this problem does not arise in the way this model is structured. It is also important to note that if the entire data is provided, the model can effectively recreate the response.

We will demonstrate the predicted response in the case of providing representative data points as input (Fig. 9) versus providing the entire experiment data (Fig. 10). With this data as the input, we will run the simulation to predict the response for the same strain routine. This strain routine includes two internal loops. It is to be noted that the internal loops are the same internal loops which were run during the experiment. For the sake of this example,(Fig. 9) only the outer hysteresis data is provided to the model, and the model is required to predict internal loops. This can be compared to the experimental data (which includes internal loops). It is to be noted that the about 60,000 hysterons (about half of which were hysterons with zero output, meaning that they did not contribute to predicting the response) were used to generate the results shown below.

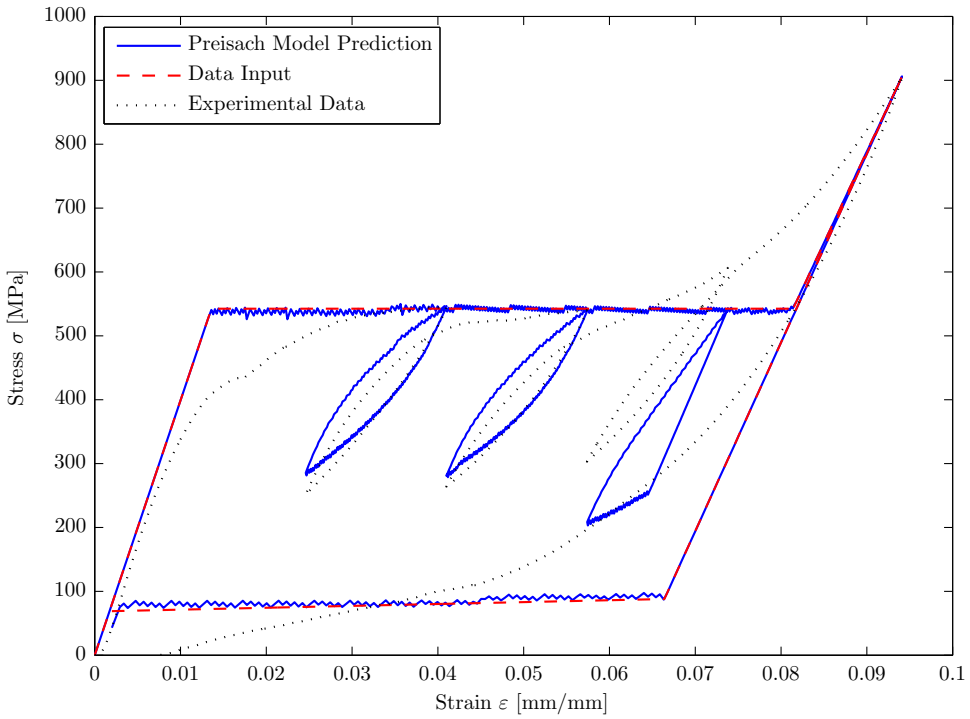

Fig. 9. The model prediction of response at 373 K of Nitinol wire. Note that the plot shows an overlay of the data given as input, the predicted response and the data that the result is compared against. In this case, it can be clearly seen that the input data is a very crude approximation of the actual experiment data.

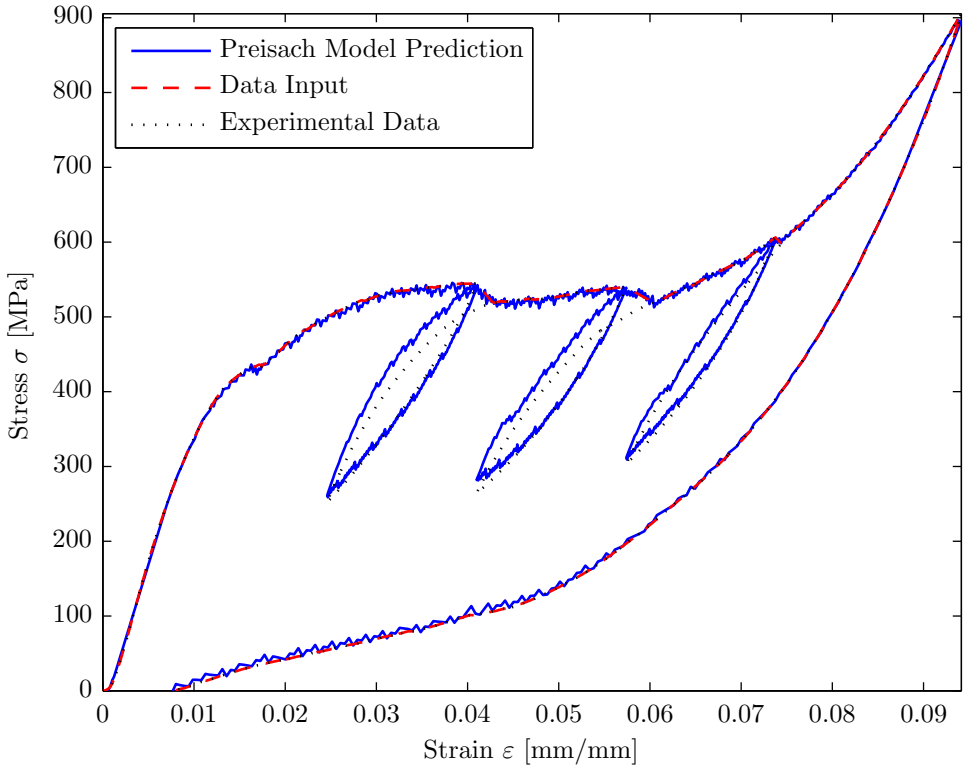

Fig. 10. The model prediction of response at 373 K of Nitinol wire. Note that the plot shows an overlay of the data given as input, the predicted response and the data that the result is compared against. In this case, the input data is the outer hysteresis extracted from the experimental data. Notice the match between the predicted internal loops and the experiment.

B. Prediction of Change in Response with Changes in Temperature

Figs. 9 and 10 both show the predicted response at the same temperature as that of the experiment (θ_1). The following set of predictions compare the response of the Preisach model based on data from temperature θ_1 and predicting response at two different temperatures θ_2 and θ_3 ($\theta_2 < \theta_1 < \theta_3$). The experiments were performed at 348 K, 373 K and 398 K. Using the outer loop of hysteresis from the experiment at 373 K, we predicted the response at 348 K and 398 K. These can be seen in Figs. 11 and 12.

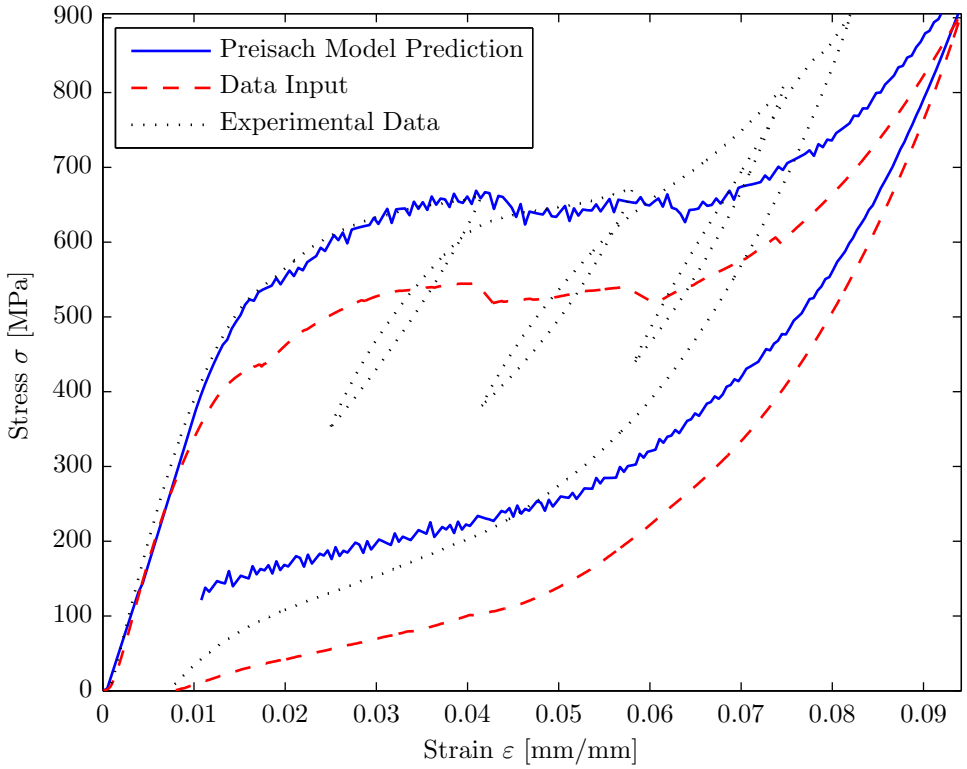

Fig. 11. The model prediction of response at 398 K of Nitinol wire, based on input data at 373 K. Notice that the model is capable of approximately predicting the response upto 6 % strain.

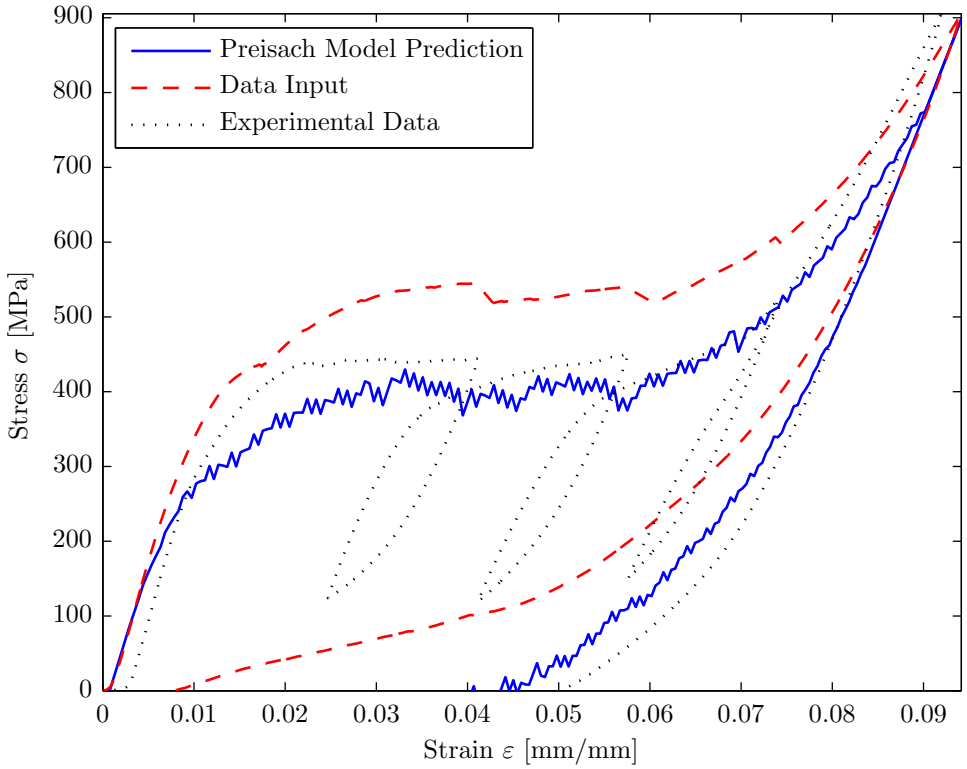

Fig. 12. The model prediction of response at 348 K of Nitinol wire, based on input data at 373 K. Notice that here again the model is able to approximately model the strain upto 6 %.

C. Discussion

The figures above show the various capabilities of the proposed Preisach model. Firstly, it can be noticed that the fidelity to the data given as input is high. Also, the proposed model is able to perform consistently well irrespective of the slopes of the upper plateau. This is useful, especially since we can then give only the salient points of the response as input. For the purposes of design, this model is thus handy, to give an idea of design values of stress at different strain values.

It can also be seen that the internal loops are characteristic of the Preisach mode, showing "return-point memory" (also known as "wiping out property"). This is one

of the features of the Preisach setup. However,the data, as can be seen in Fig. 10, does not show this property. But in essence, the area under the internal loops are well captured by the proposed model. In fact, it can be seen that even in the crude approximation for Fig. 9 shows agreement with internal loops in the experimental data. On, the other hand, the response shown in Fig. 10 models the entire experiment including internal loops with greater accuracy. This enables use of such a model for design as well as control systems.

The other important feature exhibited by the proposed Preisach model is that without any additional input, the model is able to predict the response at different temperatures given only the data from two temperatures. It can be seen that, the data was from an experiment conducted at 373 K but, the model, in Figs. 11 and 11, shows predictions at 398 K and 348 K respectively. It is to be noted that, the only data given to the model from the experiment at 398 K was the plateau stress value. It can be seen that without increasing any paramaters, or recomputing the values of the hysteron parameters, the model is able to compute the response at two other temperatures. This can indeed be extended to different temperatures.

CHAPTER VI

CONCLUSIONS

A. Summary

The model presented in this work is motivated by the need for a model which can predict internal hysteresis loops. This was accomplished by developing a thermodynamics based discrete Preisach model. The thermodynamics frameworks helps in separating the thermoelastic part of the response, and the dissipative response is modeled using the Preisach Model. The results of simulations using the model were compared with experimental data in the previous chapter.

1. Observations and Discussion

It can be seen in Fig. 9 that the model was used with the linear approximation to the experimental data as input. The internal hysteresis loops were predicted with only the global, crude linear approximation as input. It can be seen that the model prediction is quite close to the internal hysteresis loops of the experiment up to about 5%. But the model predicts a larger hysteresis loop for the third internal hysteresis loop. It can also be seen that the model does not capture the slopes during initial loading and unloading and that the curve at the onset of the plateau stress is also not predicted correctly. These results are useful for simple, design calculations, which can give an idea of the approximate stress levels, amount of dissipation and stiffness of the material when undergoing internal hysteresis loops. It can also be inferred that in this case, instead of using a horizontal line, one might use a linear approximation between the start of the plateau and the maximum strain points to get a better prediction. For use with design, one could use a linear approximation to only 5% since SMAs are

not generally used up to 10% strain in real life applications

In Fig. 10 , the data input is the global hysteresis input extracted from the experimental data. The internal hysteresis loops which are predicted show a good match with the experimental data. It can be seen that in this case, in comparison with Fig. 9, the internal loops match better with the experiment, in terms of the stiffnesses and the area of hysteresis. It is clear that when the data available is the full stress–strain response, the model is able to capture the key aspects of the response.

Fig. 11 and 12 show the model's prediction of the variation of stress–strain response with temperature. In order to predict this, the model's input was the global hysteresis at 373 K, and the variation of the driving force with temperature (assumed to be linear) is computed using the upper plateau stress under two temperatures (in this case 373 K and 398 K) as explained in Chapter IV. It can be seen that the models perform well under such a simplistic assumption, and the model shows good match with the experiments for up to 6 % in Fig. 11 as with Fig. 12.

B. Directions of Future Work

It was shown that the proposed Preisach model is able to predict the response of superelastic Shape Memory Alloys, in particular internal loops and temperature effects. Added to that, the model is also capable of predicting internal loops with very minimal information from experimental data. At this stage there are a number of directions in which further work may be done on this model. A few attempts have been made and are listed here.

1. Predicting the Bending Response from Uniaxial Response

It was intended to predict the bending response of a SMA beam using only the uniaxial response of SMA beams [41]. In this work, the beam was assumed to be under pure bending, and thus the strain in the beam was assumed to be linear, and the stress in the section was predicted using the data from the uniaxial experiment (see Fig. 13). The data used for this procedure was from experiments conducted by Rejzner et al. [2].

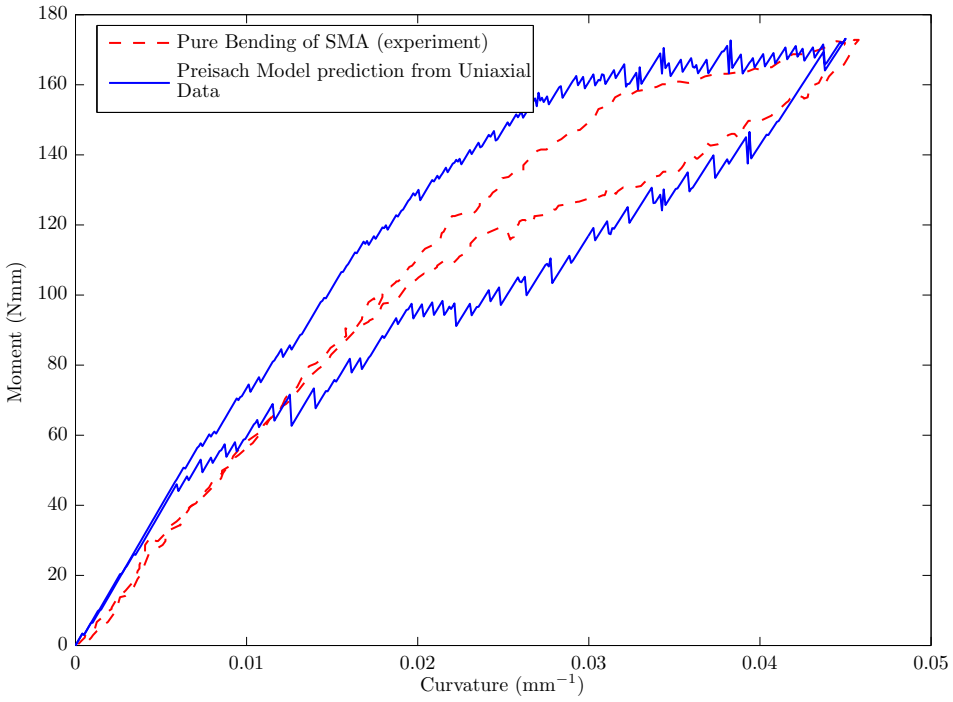

Fig. 13. Prediction of bending response of superelastic SMA beam using the experimental data from tension experiments of [2].

It is to be noted here that it was assumed that the tension and compression responses are approximately the same and that the computation of moment was done by assuming that the stress was constant in ,say, n strips (see Fig. 14) (perpendicular

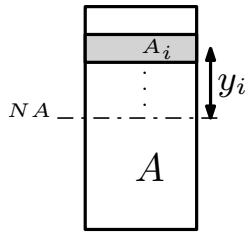

Fig. 14. Assumptions regarding computation of the moment of the SMA "beam". The cross section is divided into n strips and average stress over each of the strips is used to compute the moment at this section.

to the neutral plane) on the cross section. Indeed, increasing the number of strips n on the cross section, and data of the compression experiment of SMA will improve the prediction of bending response from the uniaxial response. It can be seen that the model largely overestimates the hysteresis. This is due to the assumptions that have been made for the strains in the beam as well as the assumption that the tensile and compressive response are the same. In addition to that, the model also computes the average stress in a few strips only (4, for the results shown in 13). In order to predict bending purely based on uniaxial response, it may be important to have better data for the uniaxial (tension and compression) response and also compute stresses at more number of strips.

2. Using Preisach Model for Shape Memory Alloy Response with Double Plateaus

Recent advances in digital image correlation (DIC) allowed research Efstathiou et al. [3] to capture double plateau corresponding to two different martensitic transformation. Under the assumptions of the model, it is to be noted that the Gibbs Potential assumes of only one kind of phase transformation taking place, whereas the authors of [3] note that two separate transformations maybe the reason for the observation of such double plateaus. A Gibbs Potential which takes into consideration this dou-

ble phase transformation, combined with appropriate corrections for the interfacial energy, would present a more physically meaningful model for such responses. Nevertheless as a testimony to the versatility of this model, we show the predicted response (with ad-hoc parameter choice) in Fig. 15.

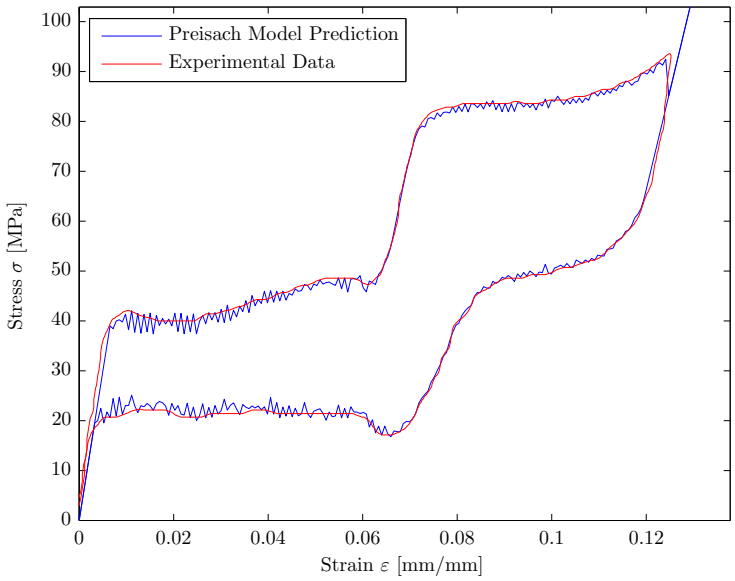

Fig. 15. Prediction of superelastic response of NiFeGa from data of [3]

C. Conclusions

To reiterate, the model's versatility is exhibited in these two examples. It is to be noted that, much of this is possible because of the separation of the thermoelastic and dissipative parts. The response was simulated using MATLAB and the discrete Preisach model setup allows for easy and fast computation. We also showed that, for the proposed model, the input need not be the entire experimental data, and even a linear approximation to the superelastic response is able to capture the internal loops of the response.

REFERENCES

[1] G. Bertotti and I. D. Mayergoyz, *The Science of Hysteresis:* 3-volume set. New York, USA: Academic Press, 2006.

[2] J. Rejzner, C. Lexcellent, and B. Raniecki, "Pseudoelastic behaviour of shape memory alloy beams under pure bending: experiments and modelling," *International Journal of Mechanical Sciences*, vol. 44, no. 4, pp. 665 – 686, 2002. [Online]. Available: http://www.sciencedirect.com/science/article/B6V49-45992SS-3/2/b3af58303b1ae1b3afdaadaa65e60461

[3] C. Efstathiou, H. Sehitoglu, J. Carroll, J. Lambros, and H. J. Maier, "Full-field strain evolution during intermartensitic transformations in single-crystal NiFeGa," *Acta Materialia*, vol. 56, no. 15, pp. 3791 – 3799, 2008. [Online]. Available: http://www.sciencedirect.com/science/article/B6TW8-4SJ4KWK-1/2/459cbd9cfa1cb082f00c2c392c6ef07f

[4] R. Smith, *Smart Material Systems: Model Development.* Philadelphia, USA: SIAM, Society for Industrial and Applied Mathematics, 2005.

[5] R. DesRoches, "Seismic retrofit of simply supported bridges using shape memory alloys," *Engineering Structures*, vol. 24, no. 3, pp. 325–332, 2002. [Online]. Available: http://linkinghub.elsevier.com/retrieve/pii/S0141029601000980

[6] K. Wilde, P. Gardoni, and Y. Fujino, "Base isolation system with shape memory alloy device for elevated highway bridges," *Engineering Structures*, vol. 22, no. 3, pp. 222–229, 2000. [Online]. Available: http://linkinghub.elsevier.com/retrieve/pii/S0141029698000972

[7] J. N. Kudva, C. A. Martin, L. B. Scherer, A. Peter Jardine, A. R. McGowan, R. C. Lake, G. P. Sendeckyj, and B. P. Sanders, "Overview of the DARPA/AFRL/NASA Smart Wing program," in *Smart Structures and Materials 1999: Industrial and Commercial Applications of Smart Structures Technologies*, J. H. Jacobs, Ed., vol. 3674. Newport Beach, CA, USA: SPIE, Jul. 1999, pp. 230–236. [Online]. Available: http://link.aip.org/link/?PSI/3674/230/1

[8] D. Stoeckel, A. Pelton, and T. Duerig, "Self-expanding nitinol stents: material and design considerations," *European Radiology*, vol. 14, no. 2, pp. 292–301, 2004. [Online]. Available: http://www.springerlink.com/content/2n6hmk3wkfx4cu4r/

[9] T. W. Duerig, A. R. Pelton, and D. Stöckel, "The utility of superelasticity in medicine," *Bio-Medical Materials and Engineering*, vol. 6, no. 4, pp. 255–266, 1996, PMID: 8980834. [Online]. Available: http://www.ncbi.nlm.nih.gov/pubmed/8980834

[10] F. Wang, W. Buehler, and S. Pickart, "Crystal Structure and a Unique "Martensitic" Transition of TiNi," *Journal of Applied Physics*, vol. 36, pp. 3232–3239, Jan. 1965. [Online]. Available: http://link.aip.org/link/?JAPIAU/36/3232/1

[11] R. Krishnan, L. Delaey, H. Tas, and H. Warlimont, "Thermoplasticity, pseudoelasticity and the memory effects associated with martensitic transformations," *Journal of Materials Science*, vol. 9, no. 9, pp. 1536–1544, Jan. 1974. [Online]. Available: http://www.springerlink.com/index/R4605Q865128752N.pdf

[12] K. Melton and O. Mercier, "The mechanical properties of NiTi-based shape memory alloys," *Acta Metallurgica*, vol. 29, pp. 39–398, Jan. 1981. [Online]. Available: http://linkinghub.elsevier.com/retrieve/pii/0001616081901656

[13] F. Auricchio, "A uniaxial model for shape-memory alloys," *International Journal of Solids and Structures*, vol. 34, no. 27, pp. 3601–3618, 1997.

[14] Z. Bo and D. C. Lagoudas, "Thermomechanical modeling of polycrystalline SMAs under cyclic loading, Part IV: modeling of minor hysteresis loops," *International Journal of Engineering Science*, vol. 37, no. 9, pp. 1205–1249, 1999.

[15] K. R. Rajagopal and A. R. Srinivasa, "On the thermomechanics of shape memory wires," *Zeitschrift für Angewandte Mathematik und Physik (ZAMP)*, vol. 50, no. 3, pp. 459–496, 1999.

[16] A. Chari, A. Garay, and R. Arróyave, "Thermodynamic remodeling of the Co-Ga system," *Calphad*, vol. 34, no. 2, pp. 189 – 195, 2010. [Online]. Available: http://www.sciencedirect.com/science/article/B6TWC-4YKDN46-1/2/9155df3ac6f95d22c651dc1df41e5c8d

[17] G. S. Firstov, J. Van Humbeeck, and Yu. N. Koval, "Comparison of high temperature shape memory behaviour for ZrCu-based, Ti-Ni-Zr and Ti-Ni-Hf alloys," *Scripta Materialia*, vol. 50, no. 2, pp. 243 – 248, 2004, viewpoint Set No. 33. Shape Memory Alloys. [Online]. Available: http://www.sciencedirect.com/science/article/B6TY2-49RCC1N-5/2/7816060cba76614e4b20b56bbde04a51

[18] P. J. S. Buenconsejo, H. Y. Kim, H. Hosoda, and S. Miyazaki, "Shape memory behavior of Ti-Ta and its potential as a high-temperature shape memory alloy," *Acta Materialia*, vol. 57, no. 4, pp. 1068 – 1077, 2009. [Online]. Available: http://www.sciencedirect.com/science/article/B6TW8-4V0V15C-4/2/307bfe6c992eb0f61891d0ff8886d529

[19] P. K. Kumar and D. C. Lagoudas, "Experimental and microstructural characterization of simultaneous creep, plasticity and phase transformation in Ti50Pd40Ni10 high-temperature shape memory alloy," *Acta Materialia*, vol. 58, no. 5, pp. 1618 – 1628, 2010. [Online]. Available: http://www.sciencedirect.com/science/article/B6TW8-4Y0656F-1/2/1235b5e824c4fbdc9bba08f33ddebfe9

[20] Y. M. Jin, "Domain microstructure evolution in magnetic shape memory alloys: Phase-field model and simulation," *Acta Materialia*, vol. 57, no. 8, pp. 2488 – 2495, 2009. [Online]. Available: http://www.sciencedirect.com/science/article/B6TW8-4VTG1PP-3/2/cfae91be6d1dfce7d3c97f5547f2b9ea

[21] H. Karaca, I. Karaman, A. Brewer, B. Basaran, Y. Chumlyakov, and H. Maier, "Shape memory and pseudoelasticity response of NiMnCoIn magnetic shape memory alloy single crystals," *Scripta Materialia*, vol. 58, no. 10, pp. 815 – 818, 2008. [Online]. Available: http://www.sciencedirect.com/science/article/B6TY2-4RJRYSK-3/2/96029d7b03bc4f1d6eee8795b7d9fc36

[22] F. Auricchio, R. L. Taylor, and J. Lubliner, "Shape-memory alloys: macromodelling and numerical simulations of the superelastic behavior," *Computer Methods in Applied Mechanics and Engineering*, vol. 146, no. 3-4, pp. 281–312, 1997.

[23] B. Raniecki and Ch Lexcellent, "Thermodynamics of isotropic pseudoelasticity in shape memory alloys," *European Journal of Mechanics - A/Solids*, vol. 17, no. 2, pp. 185–205, 1998.

[24] S. Leclercq and C. Lexcellent, "A general macroscopic description of the thermomechanical behavior of shape memory alloys," *Journal of the Mechanics and Physics of Solids*, vol. 44, no. 6, pp. 953–957, 1996.

[25] J. E. Massad and R. C. Smith, "A domain wall model for hysteresis in ferroelastic materials," *Journal of Intelligent Material Systems and Structures*, vol. 14, no. 7, pp. 455–471, 2003.

[26] F. Falk, "Ginzburg-Landau theory and solitary waves in shape-memory alloys," *Zeitschrift für Physik B Condensed Matter*, vol. 54, no. 2, pp. 159–167, 1984.

[27] J. E. Massad and R. C. Smith, "Domain wall model for SMA characterization," in *Proceedings of Smart Structures and Materials 2002: Modeling, Signal Processing, and Control*, vol. 4693, 2002, pp. 324–335.

[28] C. Liang and C. A. Rogers, "One-dimensional thermomechanical constitutive relations for shape memory materials," *Journal of Intelligent Material Systems and Structures*, vol. 1, no. 2, pp. 207–234, 1990.

[29] D. Hughes and J. T. Wen, "Preisach modeling of piezoceramic and shape memory alloy hysteresis," *Smart Materials and Structures*, vol. 6, no. 3, p. 287, 1997.

[30] J. Ortín, "Preisach modeling of hysteresis for a pseudoelastic Cu-Zn-Al single crystal," *Journal of Applied Physics*, vol. 71, pp. 1454–1461, Jan. 1992. [Online]. Available: http://link.aip.org/link/?JAPIAU/71/1454/1

[31] G. V. Webb, D. C. Lagoudas, and A. J. Kurdila, "Hysteresis modeling of SMA actuators for control applications," *Journal of Intelligent Material Systems and Structures*, vol. 9, no. 6, pp. 432–448, 1998.

[32] M. M. Khan and D. C. Lagoudas, "Modeling of shape memory alloy pseudoelastic spring elements using Preisach model for passive vibration isolation," in *Proceedings of SPIE*, 2002, pp. 336–347.

[33] A. Ktena, D. I. Fotiadis, P. D. Spanos, and C. V. Massalas, "A Preisach model identification procedure and simulation of hysteresis in ferromagnets and shape-memory alloys," *Physica B: Condensed Matter*, vol. 306, no. 1-4, pp. 84–90, 2001.

[34] I. D. Mayergoyz, "Mathematical models of hysteresis," *Physical Review Letters*, vol. 56, no. 15, p. 1518, 1986.

[35] G. Bertotti, *Hysteresis in Magnetism: For Physicists, Materials Scientists, and Engineers*, 1st ed. New York, USA: Academic Press, 1998.

[36] I. Mayergoyz, *Mathematical Models of Hysteresis*, 1st ed. New York, USA: Springer, 1990.

[37] D. H. Everett, "A general approach to hysteresis. Part 3.-A formal treatment of the independent domain model of hysteresis," *Transactions of the Faraday Society*, vol. 50, pp. 1077–1096, 1954. [Online]. Available: http://dx.doi.org/10.1039/TF9545001077

[38] J. Nealis, "Model-Based Robust Control Designs for High Performance Magnetostrictive Transducers." Ph.D. dissertation, North Carolina State University, 2003.

[39] M. Grant and S. Boyd, "CVX: Matlab Software for Disciplined Convex Programming, version 1.21," 2010. [Online]. Available: `http://cvxr.com/cvx`

[40] ——, "Graph implementations for nonsmooth convex programs," in *Recent Advances in Learning and Control*, ser. Lecture Notes in Control and Information Sciences, V. Blondel, S. Boyd, and H. Kimura, Eds. New York, USA: Springer-Verlag Limited, 2008, pp. 95–110.

[41] S. Doraiswamy and A. Srinivasa, "A thermodynamics based discrete Preisach model to predict the bending response of SMA wires using uniaxial data," in *USNCTAM 2010 Conference Proceedings*, 2010.

APPENDIX A

MATLAB IMPLEMENTATION OF THE MODEL

The structogram shown below is the pseudocode for the simulation explained in Chapter IV.

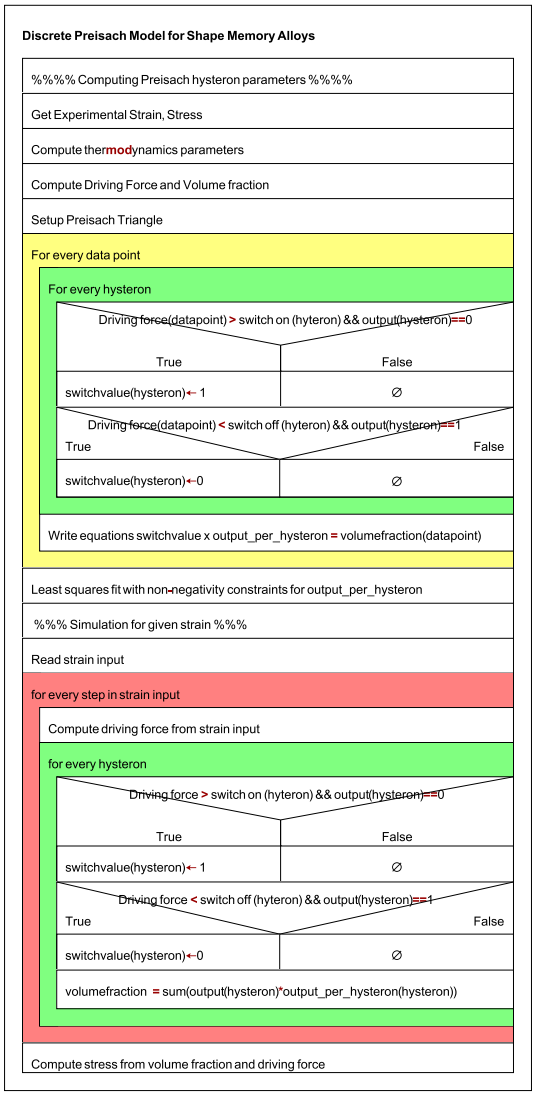

Fig. 16. Structogram for the computer simulation of the proposed model.

This appendix is a compilation of the various subroutines which are used in the computer simulation of the model.

main.m

```
%+++++++++++++++++++++++++++++++++++++++++++++++++++++++++++++++
% Run this code to generate results for Modified Preisach
% for response under tension
%+++++++++++++++++++++++++++++++++++++++++++++++++++++++++++++++
clear all
clc
tic
%============================
% Number of Preisach Levels
%============================
Nlevels = 350;
%================================================
% Number of load steps per leg of strain_input
%================================================
Nsteps_per_leg =200;
%================
% Strain input
%================
strainendpoints =[0,0.041,0.0246,0.06,0.002];
%================================
% Strain Input from function
%================================
strain_input = GetInputVector(strainendpoints,Nsteps_per_leg);
%====================================
% Total Number of load steps
%====================================
Nsteps = length(strain_input);
%=================
% Filename for data
%=================
filename = 'ashwin_sample23_outer.dat';
inputpointdata = 'ashwin_sample23.mat';
%=========================================================
%Calculate the forward and backward switches for the Preisach Elements
%=========================================================
[df_forward df_backward vfmax_per_ele] =
CalculatePreisachSwitches(filename,Nlevels);
%=========================================
% Compute stress for the given strain
%=========================================
[stress_predicted_classical,strain_input,F_classical,vf_classical]
= RunPreisach(df_forward,df_backward,vfmax_per_ele,...
strain_input,Nlevels,Nsteps,filename);
```

```
%=======================================
% Plotting the stress strain curve
%=======================================
close all
data=load(filename);
plot(strain_input,stress_predicted_classical,'b',...
data(:,1),data(:,2),'r')
```

GetInputVector.m

```
function vector_input = GetInputVector(endpoints,Nsteps_per_leg)
% To generate the vector_input vector using linspaces
vector_input=[];
Nendpoints = length(endpoints);
for i = 1:Nendpoints-1
    vector_input
= [vector_input,...
linspace(endpoints(i),endpoints(i+1),Nsteps_per_leg)];
end
```

CalculatePreisachSwitches.m

```
function [df_forward df_backward vfmax_per_ele]
= CalculatePreisachSwitches(filename,Nlevels)
% INPUT VARIABLES
%     Nlevels - Number of levels in the Preisach Triangle
% OUTPUT VARIABLES
%     df_forward - Forward direction switch
% for Preisach Element (Nlevels x 1)
%     df_backward - Forward direction switch\
%  for Preisach Element (Nlevels
%     x 1)
%     vfmax_per_ele - Maximum Volume fraction
% yield per Preisach Element
%============================
% Initialization
%============================
flag_ele = zeros(Nlevels);
Amat = zeros(Nlevels,Nlevels^2);
Bvec = zeros(Nlevels,1);
%================================================
% Finding the driving force and volume fraction
```

```
%=================================================
[drivingforce,volumefraction] = Resampling(filename,Nlevels);
%=================================================
% Forward and Backward switches for each element
%=================================================
df_forward = linspace(min(drivingforce),...
max(drivingforce),Nlevels);
df_backward = linspace(min(drivingforce),...
max(drivingforce),Nlevels);
%=================================================================
% Setting the switch values in element positions in the triangle
%=================================================================
df_forward_matrix = sparse(tril...
(repmat(df_forward',1,Nlevels)));
df_backward_matrix = sparse(tril...
(repmat(df_backward,Nlevels,1)));
%=========================================================
% Initializing df_forward & df_backward for later storage
%=========================================================
df_forward=zeros(1,Nlevels^2);
df_backward=zeros(1,Nlevels^2);
%=========================================================
% Setting up equations to be solved to find vfmax_per_ele
%=========================================================
%------------------------------
% For each step of driving force,
%------------------------------
for step = 2 : Nlevels
%-----------------------------------------------------------------
% Check if the driving force will switch on the element or not
%-----------------------------------------------------------------
    if drivingforce(step) > drivingforce(step-1)
        drivingforcetemp = drivingforce(step);
        %------------------------------
        % For each element coordinate,
        %------------------------------
        for i = 1 : Nlevels
            for j = 1 : i
                if drivingforcetemp >= df_forward_matrix(i,j)
                    if flag_ele(i,j) == 0
                        flag_ele(i,j) = 1;
                    end
                end
            end
        end
    else
        %------------------------------
        % For each element coordinate,
        %------------------------------
        for i = 1 : Nlevels
            for j = 1 : i
```

```
                if drivingforce(step) <= df_backward_matrix(i,j)
                     if flag_ele(i,j) == 1
                         flag_ele(i,j) = 0;
                     end
                 end
             end
         end
    end
%-------------------------------------------------------
% Assign the flags as a row of
% the A matrix for least squares (Ax=B)
%
% Converting elements of flag_ele to elements of Amat
%                                 (matrix of coefficients)
%and writing df_forward, df_backward in a usable fashion
%-------------------------------------------------------
    Amat(step,:) = flag_ele(:);
    df_forward(1,:) = df_forward_matrix(:);
    df_backward(1,:) = df_backward_matrix(:);
    Bvec(step,1) = volumefraction(step);
end
%==============================
% Solving for vfmax_per_ele
%==============================
Amat = sparse(Amat);
n = Nlevels^2;
cvx_begin quiet
    variable vfmax_per_ele(n);
    minimize( norm(Amat*vfmax_per_ele-Bvec) );
    subject to
        vfmax_per_ele >= 0;
cvx_end
```

Resampling.m

```
function [df_resampled,vf_resampled]=Resampling(filename,Nlevels)
% INPUT VARIABLES
%     drivingforce - Nondimensionalized driving force
%     volumefraction - Nondimensionalized volume fraction
%     Nlevels - Number of levels in the Preisach triangle
% OUTPUT VARIABLES
%     df_resampled - Resampled drivingforce, with size Nlevels
%     vf_resampled - Resampled volumefractio, with size Nlevels
%================================================
% Finding the driving force and volume fraction
%================================================
[drivingforce,volumefraction] = DrivingForceVolumeFraction(filename);
```

```
%=================
% Computing sizes
%=================
length_df = length(drivingforce);
length_vf = length(volumefraction);
%=============
% Resampling
%=============
dftemp = drivingforce;
vftemp = volumefraction;
df_resampled = ChangeLength(dftemp,Nlevels);
vf_resampled = ChangeLength(vftemp,Nlevels);
for i = 1:length(vf_resampled)
    if vf_resampled(i) < 0
        vf_resampled(i) = 0;
    end
end
```

DrivingForceVolumeFraction.m

```
function [drivingforce,volumefraction]=
DrivingForceVolumeFraction(filename)
% INPUT VARIABLES
%     filename - name of the file with data
%     material - name of the material type
% OUTPUT VARIABLES
%     drivingforce - Nondimensionalized driving force
%     volumefraction - Nondimensionalized
% volume fraction of martensite
%=========================================================
% Get the nondimensionalized stress and strain from file
%=========================================================
[stress,strain] = GetStressStrain(filename);
%==================
% Nondimensionalized Temperature
%==================
T = 1;
%=============================================
% Compute driving force and volume fraction from
% the stress and strain
%=============================================
load ashwin_sample23.mat
params = GetParams(inputdata);
E_a = params.E(1);
E_m = params.E(2);
B = params.B;
a = params.thermal(1);
```

```
b = params.thermal(2);
volumefraction = ( strain - (stress.*inv(E_a)) ) ./ ...
( stress.* (inv(E_m) - inv(E_a)) + 1);
for i=1:length(volumefraction)
    if volumefraction(i)<0
        volumefraction(i) = 0;
    end
end
drivingforce = stress.^2.*(inv(2*E_m) - inv(2*E_a))
 - B.*( 2.*volumefraction-1 )+ a + b * T  + stress;
```

GetParams.m

```
function params = GetParams(inputdata)
% Parameters from the Gibbs Potential
coords=inputdata.coords; % 7 points input as per ASTM standards
temp_exp = inputdata.temp_exp1;
temp_exp2 = inputdata.temp_exp2;
stress_ref = 0.5*(coords(1,2)+coords(2,2));
strain_ref = coords(3,1);
E_a = (strain_ref/stress_ref)*(coords(1,2)/coords(1,1));
E_m = (strain_ref/stress_ref)*((coords(4,2)-coords(3,2))/...
(coords(4,1)-coords(3,1)));
B=trapz([0;coords(1:5,1)]/strain_ref,[0;coords(1:5,2)]/stress_ref);
stress_ref_exp2 = 0.5*(coords(6,2)+coords(7,2));
thermalslope=polyfit([temp_exp2,temp_exp],...
[stress_ref_exp2,stress_ref],1);
b=-thermalslope(1);
a=2*(-b);
params.reference = [stress_ref strain_ref temp_exp];
params.E = [E_a E_m];
params.B = -B;
params.thermal = [a b];
```

GetStressStrain.m

```
function [stress,strain]=GetStressStrain(filename)
% INPUT VARIABLES
%     filename - name of data file
% OUTPUT VARIABLES
%     stress - nondimensionalized stress from data
```

```
%     strain - nondimensionalized strain from data
%============================
% Extract data from the file
%============================
load ashwin_sample23.mat
params = GetParams(inputdata);
data = dlmread(filename);
strain = data(:,1)/params.reference(2);
stress = data(:,2)/params.reference(1);
```

ChangeLength.m

```
function [resampled] = ChangeLength(vector,changetolength)
% INPUT VARIABLES
%     vector - The vector to be resized
%     changetolength - The length of desired output
% OUTPUT VARIABLES
%     resampled - Gives the output of length changetolength
resampled = zeros(changetolength,1);
changetolength=changetolength+1;
lengthofinput = length(vector);
% Length of averaging window
windowsize = ceil(lengthofinput/changetolength);
k=1;
for i=1:windowsize:lengthofinput-windowsize
    resampled(k) = mean(vector(i:i+windowsize-1));
    k=k+1;
end
```

RunPreisach.m

```
function [stress_predicted,strain_input,F,vf]
 = RunPreisach(df_forward,df_backward,vfmax_per_ele,...
strain_input,Nlevels,Nsteps,filename)
% INPUT VARIABLES
%     df_forward - List of the switch values
% for the hysterons in the forward direction
%     df_backward - List of the switch values
% for the hysterons in the backward direction
%     vfmax_per_ele - The maximum possible
% volume fraction yield per hysteron
%     strain_input - Input strain for which
```

```
% predicted stress is required
%     Nlevels - Number of levels in the Preisach Triangle
%     Nsteps - Number of loading steps in strain_input
% OUTPUT VARIABLES
%     stress_predicted - Predicted Stress (Classic Preisach)
%=====================
% Initialization
%=====================
stress_nd = zeros(Nsteps,1);
vf = zeros(Nsteps,1);
F = 2*ones(Nsteps,1);
Nele = Nlevels^2;
hysteron = zeros(Nlevels);
%================================
% Getting parameters
%================================
load ashwin_sample23.mat
params = GetParamsUpdated(inputdata);
E_a = params.E(1);
E_m = params.E(2);
B=params.B;
a=params.thermal(1);
b=params.thermal(2);
stress_ref = params.reference(1);
strain_ref = params.reference(2);
temp_ref = params.reference(3);
strain_nd = strain_input/strain_ref;
%==================
% Get temperature
%==================
T_orig = GetTemperature(filename);
T = T_orig/temp_ref;
%====================
% (1/E_m - 1/E_a)
%====================
diff_inv_moduli = (1/E_m - 1/E_a);
% _____________________________________________________%

%++++++++++++++++++++++++++++++++++++++++++++++++
% Run the Preisach algorithm for the setup
%++++++++++++++++++++++++++++++++++++++++++++++++
%=================
% For each step
%=================
for step = 2:Nsteps
    if strain_nd(step-1) == 0
        vf(step-1) = 0;
    end
    stress_nd(step) = (strain_nd(step) - vf(step-1)) /...
( vf(step-1) * diff_inv_moduli + inv(E_a) );
    F(step) = stress_nd(step) + 0.5*stress_nd(step)^2*...
```

```
diff_inv_moduli - B*(2*vf(step-1)-1) + a + b*T;
    Ftemp = F(step);
    for ele = 1:Nele
        if vfmax_per_ele(ele) > 0
            if Ftemp <= df_backward(ele) && hysteron(ele) == 1
                hysteron(ele) = 0;
            elseif Ftemp > df_forward(ele) && hysteron(ele) == 0
                hysteron(ele) = 1;
            end
        end
    end
    vf(step) = sum(hysteron(:).*vfmax_per_ele(:));
    stress_nd(step) = (strain_nd(step)-vf(step))/...
(vf(step)/E_m + (1-vf(step))/E_a);
    F(step) = stress_nd(step) + 0.5*stress_nd(step)^2*...
diff_inv_moduli - B*(2*vf(step)-1) +a +b*T;
end
stress_predicted = stress_ref*stress_nd;
```

GetTemperature.m

```
function T=GetTemperature(filename)
% INPUT VARIABLES
%     material - material type
% OUTPUT VARIABLES
%     T - Temperature of operation
switch filename
    case 'ashwin_sample23_outer.dat'
       T = 373;
    case 'ashwin_sample24_outer.dat'
        T = 398;
    case 'ashwin_sample25_outer.dat'
        T = 348;
    case 'linear23.dat'
        T=373;
    case 'linear24.dat'
        T=398;
    otherwise
        error('Unknown Material Type')
end
```

VITA

Name : Srikrishna Doraiswamy

Address : c/o Dr. Arun R. Srinivasa,
Department of Mechanical Engineering,
Texas A&M University
College Station,TX 77843-3123

Email Address : srikrishna.doraiswamy@gmail.com

Education : *M.S. Mechanical Engineering*, Texas A&M University,
College Station, TX, 2010
B.Tech. Civil Engineering, Indian Institute of Technology Madras,
Chennai, India, 2008